The Journal of Physical Chemistry A

 VOLUME 101, NUMBER 31, JULY 31, 1997

ARTICLES

Kinetic Study of Inelastic Collisions of NH/ND($c^1\Pi$,v,J) with O_2: Rotational and Vibrational Relaxation, Quenching, and Intersystem Crossing

J. Hohmann† and F. Stuhl*

Physikalische Chemie I, Ruhr-Universität Bochum, D-44780 Bochum, Germany

Received: February 21, 1997; In Final Form: May 22, 1997[⊗]

We have studied the fate of selectively excited vibrational and rotational NH/ND($c^1\Pi$,v,J) states in inelastic collisions with O_2. The excited states were produced in a two-step procedure by first photolyzing hydrazoic acid to yield NH/ND(a), which then was excited to the c state. This work presents rate data for rotational relaxation in the c,v=0 states, overall quenching of rotational states, intersystem crossing to the $A^3\Pi$ state, vibrational relaxation of the ND(c,v=1) state, and quenching of the vibrational ND(A,v=0−3) states. Additionally the vibrational distributions of the A state products were determined as a function of rotation of the c states.

Introduction

The collision-induced singlet−triplet intersystem crossing $c^1\Pi \rightarrow A^3\Pi$ of the NH radicals has been reported for the first time by Okabe.[1] In the VUV (vacuum-ultraviolet) photolysis of HN_3, he observed a decreasing intensity of the singlet NH($c^1\Pi \rightarrow a^1\Delta$) fluorescence upon the addition of O_2 and NO, while the triplet NH($A^3\Pi \rightarrow X^3\Sigma^-$) emission intensity increased. Okabe proposed the spin-allowed, exothermic reactions

$$\mathrm{NH}(c^1\Pi) + \mathrm{O_2}(X^3\Sigma_g^-) \rightarrow \mathrm{NH}(A^3\Pi) + \mathrm{O_2}(a^1\Delta_g); \quad \Delta_r H = -68\ \mathrm{kJ\ mol^{-1}} \qquad \text{(Ia)}$$

$$\rightarrow \mathrm{NH}(A^3\Pi) + \mathrm{O_2}(b^1\Sigma_g^+); \quad \Delta_r H = -5.3\ \mathrm{kJ\ mol^{-1}} \qquad \text{(Ib)}$$

and the total spin-changing reaction

$$\mathrm{NH}(c^1\Pi) + \mathrm{NO}(X^2\Pi) \rightarrow \mathrm{NH}(A^3\Pi) + \mathrm{NO}(X^2\Pi); \quad \Delta_r H = -162\ \mathrm{kJ\ mol^{-1}} \qquad \text{(II)}$$

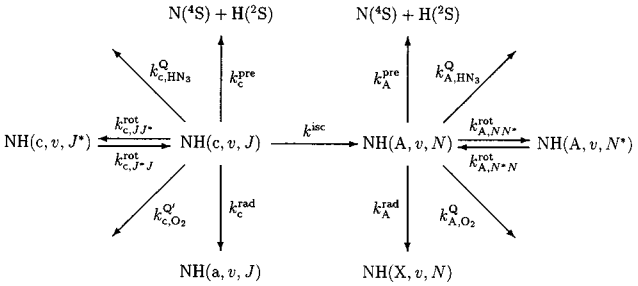

Figure 1. Reaction scheme of the relevant processes in the system NH(c,v=0) + O_2 → NH(A) + O_2. Vibrational energy transfer, radiative NH(c→b) transitions, and transitions between different Λ-doublet states are not considered in this scheme. For ND a similar scheme is valid.

to be responsible for the effective conversion. Quenching by HN_3 was not considered in that work, and rate constants and efficiencies of the processes were estimated on the basis of the NH(c) lifetimes and quenching rate constants available then.

Subsequently, Kawasaki et al.[2] have measured cross sections for the electronic quenching and intersystem crossing of NH(c) and ND(c) by He, Ar, Kr, and Xe and the molecular collision partners H_2, N_2, and NH_3. They found significant intersystem crossing only for Xe. The cross section for ND(c) was measured to be larger than that for NH(c).

In time-resolved and spectrally resolved experiments, Rohrer and Stuhl[3] have previously investigated the intersystem crossing

† Present address: F. Hoffmann-La Roche Ltd., Pharmaceutical Division, CH-4070 Basel, Switzerland.

⊗ Abstract published in *Advance ACS Abstracts*, July 1, 1997.

S1089-5639(97)00647-6 CCC: $14.00

of NH(c) in the presence of O_2, NO, Xe, and N_2O. They reported high intersystem crossing efficiencies for O_2 and NO and smaller ones for Xe and N_2O. In the presence of O_2, vibrationally excited NH(A,v) was found to be generated. Rate constants were determined from the comparison of the experimental with simulated intensity ratios of the singlet and triplet emissions. Photolytically generated triplet emission complicated the evaluation of the intensities.

Thereafter, Umemoto et al.[4] have performed experiments on the intersystem crossing of NH(c,v=0) in the presence of Xe, Kr, NO, O_2, and N_2O. These authors have produced the excited radicals in a two-step excitation scheme comparable to that used in this work, but only for the rotational levels $J = 2$ and 3. Different from the two-laser experiment of this work, a single laser was used to generate NH(a) and, during the same laser pulse, to excite NH(c). These authors report the efficiencies for intersystem crossing to be half of and significantly larger than those observed by Rohrer and Stuhl[3] for O_2 and Xe, respectively. No dependence on J or the nature and pressure of added gas was observed.

It is well-known that the kinetics of *quenching* of electronically excited hydrides can be dependent on the rotational state.[5] However besides the work by Umemoto et al.,[4] no *intersystem crossing* (ISC) study has been reported for selectively excited levels of NH(c,v=0,J), and it is unknown which effect rotation will have on the kinetics. The original aim of this study hence is to prepare various NH(c,v=0,J) states in the presence of O_2 and investigate the formation of triplet NH(A,v,N) states. Because of the significantly different vibrational and rotational energy spacing in the ND isotopomer, we further include ND(c,v=0,1,J). Unfortunately efficient predissociation[6] makes it impossible to perform similar experiments with vibrationally excited NH(c,v=1).

In practice, the experiments and their interpretation turned out to be rather complex due to a number of competing processes occurring after the generation of a single excited NH/ND(c,v,J) state. Figure 1 presents this problem for NH(c,v=0,J) in the presence of O_2, the collider of interest in this work. Save ISC, NH/ND(c,v,J) will undergo predissociation, radiation, rotational relaxation, and quenching by O_2 and the parent molecule HN_3 (DN_3) leading to other than triplet A states. Fortunately, quenching by HN_3 (DN_3) can be reduced at low parent pressures to become insignificant; all other processes are inherent to this system. The rotational dependence of the radiative and predissociative transitions has been recently studied experimentally and theoretically,[6] but state-resolved rate constants of rotational relaxation and quenching by O_2 are not known. Besides the quenching and ISC efficiencies, they will be determined in this work, too. As will be discussed later, the relative efficiencies for relaxation and quenching are very important to this work, because they determine whether the quenching (including ISC) can be attributed to a single, isolated rotational state or a more or less relaxed distribution of rotational levels.

Similar to NH(c), the NH(A) product of the intersystem crossing decays by a number of different channels. These processes are included in Figure 1. With the available knowledge on the NH(A) removing processes,[5,7,8] we will attempt in this work to estimate approximate internal energy distributions of the triplet products.

Experimental Section

The experimental setup has been described recently in detail,[9,10] and only the major features and modification will be given here. Population in single rotational states of excited imidogen radicals was created in a two-step absorption procedure: First metastable NH/ND($a^1\Delta$) radicals were produced in the repetitive (5−10 Hz) KrF laser (248 nm) photolysis of hydrazoic acid[11] diluted with the collision partner, oxygen. A pulsed tunable dye laser was fired 20 μs delayed after the KrF laser to form electronically excited NH/ND($c^1\Pi$,v'=0,J) by pumping on one of the isolated P- or Q-branch lines of the NH/ND($c^1\Pi$,v'=0 ← $a^1\Delta$,v''=1) transition[6] in the range 363−368 nm for NH and 351−356 nm for ND. ND(c,v=1) was produced by pumping on the corresponding (1,2) band transitions at 358−363 nm. The delay was sufficiently long to rotationally and translationally relax the NH(a) radicals even at the lowest pressures used (50 Pa). This was demonstrated for rotation by taking LIF spectra. The delay time was limited by the rapid reaction of the metastable imidogen radicals with hydrazoic acid ($k \approx 1.1 \times 10^{-10}$ cm^3 s^{-1}).[12] The rotational and vibrational population distributions of NH/ND(c,v,J) and NH/ND(A,v,N) were monitored with a 0.5 m monochromator (Minuteman, 305 M, blaze wavelength 300 nm) by the fluorescence of the respective singlet ($c^1\Pi \rightarrow a^1\Delta$) and triplet ($A^3\Pi \rightarrow X^3\Sigma^-$) transitions in the wavelength range 320−350 nm. Because of the different wavelength regions for excitation and detection, the fluorescence spectra are essentially free of stray light, and the gate of detection was set to include the whole decay curve of the fluorescence emission.

The fluorescence spectra were taken at spectral resolutions ranging from 0.05 to 0.8 nm. For each wavelength increment, the signals from about 30 laser shots were averaged by a gated integrator (EG&G PAR 4152). The spectra were digitally recorded. Each spectrum was taken at least four times to check the reproducibility.

Fluorescence decay times were measured by a digital storage oscilloscope (Le Croy 9400) at 10 ns dwell time. The decay was monitored as long as 5 μs. To determine decay rates, an interval of 3−4 lifetimes was evaluated, typically 0.2−1 μs. For each decay curve, 500−1000 laser shots were fired. Five to ten decay curves were averaged for the determination of a decay time at a given experimental condition. All error limits given in this work represent 3σ.

A number of experiments were performed to check whether the polarization of the dye laser influences the measured spectral intensities or decay rates. For this purpose, the ratio of the spectral detection sensitivity for light being polarized parallel and perpendicular to the grooves of the grating was determined in the region of the detected fluorescence. Between 320 and 350 nm it was measured to be about 1.15. Furthermore, the plane of polarization of the laser was rotated by 90° with no effect on the observed quantities. Both results are not surprising, because (i) the monochromator does not polarize light at the blaze angle and (ii) saturated laser induced fluorescence, as used in these experiments, is expected to be largely unpolarized.[13]

HN_3 and DN_3 were produced as described before.[9,11] The oxygen sample had a stated (Messer-Griesheim) purity of better than 99.99%. Mixtures of hydrazoic acid and oxygen were flowed through the photolysis cell at a constant hydrazoic acid pressure of 0.2 Pa and various pressures of O_2 ranging from 50 to 500 Pa. All experiments were performed at room temperature (≅300 K).

Results

(a) Electronic Quenching of NH/ND(c,v=0,J). Overall quenching rates due to collisions of rotationally excited NH/ND(c,v=0,J) with O_2 were obtained from time-resolved fluorescence intensity measurements. The decays of NH(c,v=0) and ND(c,v=0) radicals were monitored in the wavelength

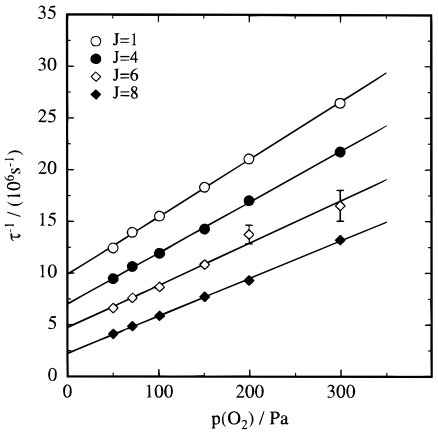

Figure 2. Decay rates of NH(c,v=0,J), τ^{-1}, as a function of O_2 pressure at 300 K. The data for J=6, J=4, and J=1 are shifted by $+2.5 \times 10^6$ s^{-1}, $+5 \times 10^6$ s^{-1}, and $+7.5 \times 10^6$ s^{-1}, respectively. The pressure of HN_3 was constant at 0.2 Pa.

TABLE 1: Rate Constants at Room Temperature for the Quenching of NH/ND(c,v=0,1,J) by O_2, k^Q_{c,O_2} ($=k^{isc} + k^{Q'}_{c,O_2}$; see Figure 1), as a Function of the Originally Excited Rotational State J

	$k^Q_{c,O_2}/(10^{-11}$ cm^3 s$^{-1})$		
	NH(c,v=0)		ND(c,v=0)
J	this work	Crosley et al.[a]	this work
v=0			
1	24.2 ± 2.4		12.0 ± 1.7
2	22.0 ± 0.4	8.2 ± 1.7	12.1 ± 0.4
3	21.2 ± 1.3		11.0 ± 0.6
4	19.7 ± 0.1		11.1 ± 0.4
5	18.5 ± 0.3		10.9 ± 0.5
6	17.2 ± 0.2	6.2 ± 2.0	11.0 ± 0.7
7	15.2 ± 0.5		10.6 ± 0.5
8	15.0 ± 0.2		11.2 ±0.3
9			10.2 ± 0.4
10		7.2 ± 2.4	
14		5.8 ± 2.2	
v=1			
1			19 ± 4

[a] Reference 20.

ranges 326 ± 3 and 325 ± 3 nm, respectively, thus comprising the P-, Q-, and R-branch lines of the (c → a) emission of all populated rotational levels ($1 \le J \le 8$ for NH and $1 \le J \le 9$ for ND). The decay of the initially populated ND(c,v=1,J=1) was measured at 332 ± 2 nm. Care was taken to avoid emission from NH/ND(A). In all cases, the intensities were found to decrease by single-exponential decays. The decay rates were linearly dependent on the pressure of oxygen. There was no indication of reverse reactions regenerating NH/ND(c). Examples of plots of decay rates vs oxygen pressure are shown in Figure 2 for NH(c,v=0,J=1,4,6,8). Quenching rate constants were obtained from the slopes of these plots as determined from least squares fits. The rate constants are summarized in Table 1.

(b) Intersystem Crossing. Vibrational distributions in NH(A) produced by ISC were inferred from the intensities of the fluorescence spectra of the NH/ND($A^3\Pi,v \rightarrow X^3\Sigma^-,v$) transitions. Examples of such spectra are shown in Figure 3 for the excitation of NH(c,v=0,J=1−5). Similar spectra were obtained for the excitation of single rotational states of ND(c,v=0,1). O_2 pressures of about 100 Pa were found to be optimal with regard to sufficient A state generation and minimum relaxation. Because of the overlapping Δv=0 bands, triplet spectra were simulated[9,14] using spectroscopic data as given by Brazier et al.[15] and Patel-Misra et al.[16] and fitted to the experimental ones

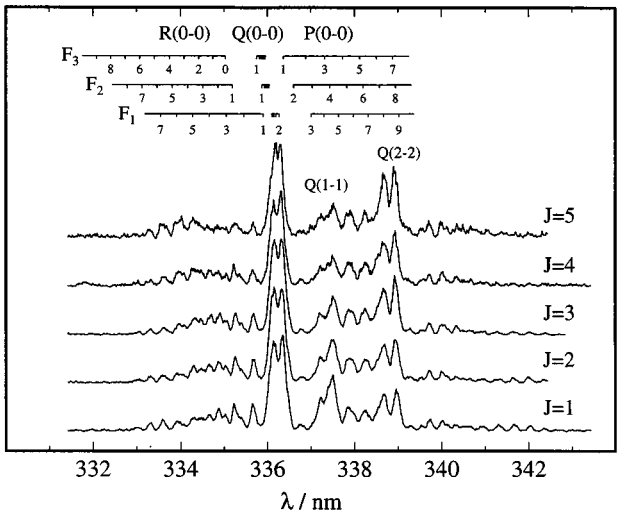

Figure 3. Fluorescence spectra of the triplet NH($A^3\Pi \rightarrow X^3\Sigma^-$) transition caused by excitation of selected rotational levels J of NH($c^1\Pi,v$=0,J). The pressures of HN_3 and O_2 were 0.2 and 104 Pa, respectively. The spectral resolution was 0.15 nm.

by visual comparison particularly of the intensities of the Q-branches to obtain relative populations of the vibrational A states. The rotational distributions adopted for the simulations were represented by the rotational temperature of 300 K for v>0 and, for v=0, by various distributions centered at the originally excited rotational state J. The vibrational distributions are obtained mainly from the shape of the congested Q-branches. They provide trends rather than accurate values. The relative vibrational populations thus derived are presented in Table 2. For ND(c,v=0,J), only the vibrational ground state ND(A,v=0) was detected independent of the initial rotational level J.

To determine the rate constants of the intersystem crossing, all removal and production channels, which are given in Figure 1, must be considered. In addition for the ND(c,v=1) + O_2 system, vibrational relaxation has to be taken into account. Notwithstanding the rotational relaxation, the decay of the NH(c) state population is determined by

$$\frac{d[NH(c)]}{dt} = -(k_c^{rad} + k_c^{pre} + k^Q_{c,HN_3}[HN_3] + (k^{isc} + k^{Q'}_{c,O_2})[O_2])[NH(c)] \quad (1)$$

This equation disregards reverse ISC. As explained above, no indication for the reverse process is observed in the time-resolved experiments, although the possible formation of NH(A,v=2) + O_2(a,v=0) in reaction Ia is close to thermoneutral. Apparently the deactivation of NH(A,v=2) by ground state O_2(X) ($k = 8.3 \times 10^{-11}$ cm^3 s^{-1})[3] is fast at the present O_2 pressures compared to the reverse ISC at the low concentration of metastable O_2(a,v=0) formed in reaction Ia.

Similarly, the time dependence of the NH(A) product concentration is given by the difference of the production and removal terms:

$$\frac{d[NH(A)]}{dt} = k^{isc}[O_2][NH(c)] - (k_A^{rad} + k_A^{pre} + k^Q_{A,HN_3}[HN_3] + k^Q_{A,O_2}[O_2])[NH(A)] \quad (2)$$

For the ND system, the same equations can be formulated. Solving these differential equations for the initial condition $[NH(A)]_{t=0} = 0$ and integrating over the whole emission time yields

TABLE 2: Relative Vibrational Populations of NH/ND($A^3\Pi$,v) Formed in the Intersystem Crossing from NH/ND($c^1\Pi$,v,J) + O_2

	NH(c,v=0,J)			ND(c,v=1,J)[a]			
J	NH(A,v=0)	NH(A,v=1)	NH(A,v=2)	ND(A,v=0)	ND(A,v=1)	ND(A,v=2)	ND(A,v=3)
1	0.48	0.24	0.28	0.20	0.42	0.20	0.18
2	0.45	0.20	0.35	*b*			
3	0.43	0.17	0.40				
4	0.43	0.13	0.44	0.21	0.39	0.20	0.20
5	0.42	0.08	0.50				
6	0.42	0.04	0.54				
7	0.41	0.02	0.57				

[a] For the deactivation of ND(c,v=0,J) only the vibrational ground state ND(A,v=0) was observed as a product independent of the initially excited J. [b] These values were not measured.

$$\frac{\int_0^\infty [\mathrm{NH(c)}]_t \mathrm{d}t}{\int_0^\infty [\mathrm{NH(A)}]_t \mathrm{d}t} = \frac{k_\mathrm{A}^\mathrm{rad} + k_\mathrm{A}^\mathrm{pre} + k_{\mathrm{A,HN_3}}^\mathrm{Q}[\mathrm{HN_3}] + k_{\mathrm{A,O_2}}^\mathrm{Q}[\mathrm{O_2}]}{k^\mathrm{isc}[\mathrm{O_2}]} \quad (3)$$

The HN_3 pressure is very small in these experiments (0.2 Pa); therefore we neglect the term $k_{\mathrm{A,HN_3}}^\mathrm{Q}[\mathrm{HN_3}]$. The gate was set to monitor the triplet and singlet emissions from $t = 0$ to four lifetimes, hence covering the whole decays. The ratio of the integrated c and A state concentrations, N_c and N_A, respectively, is thus given by

$$\frac{N_\mathrm{c}}{N_\mathrm{A}} = \frac{\int_0^\infty [\mathrm{NH(c)}]_t \mathrm{d}t}{\int_0^\infty [\mathrm{NH(A)}]_t \mathrm{d}t} = \frac{k_{\mathrm{A,O_2}}^\mathrm{Q}}{k^\mathrm{isc}} + \frac{k_\mathrm{A}^\mathrm{rad} + k_\mathrm{A}^\mathrm{pre}}{k^\mathrm{isc}} \frac{1}{[\mathrm{O_2}]} \quad (4)$$

$N_\mathrm{c}/N_\mathrm{A}$ is proportional to the ratio of the corresponding time-integrated intensities, as measured by the gated integrator. This ratio was determined for different oxygen pressures by visually fitting simulated spectral intensities of the NH/ND($c^1\Pi \rightarrow a^1\Delta$) and NH/ND($A^3\Pi \rightarrow X^3\Sigma^-$) transitions to the intensities of the observed fluorescence spectra. Typical results of plots $N_\mathrm{c}/N_\mathrm{A}$ vs $[O_2]^{-1}$ are displayed in Figure 4.

From fits of straight lines to the data of this figure, values of the ratio $(k_\mathrm{A}^\mathrm{rad} + k_\mathrm{A}^\mathrm{pre})/k^\mathrm{isc}$ were determined. With the known values of $k_\mathrm{A}^\mathrm{rad}$ and $k_\mathrm{A}^\mathrm{pre}$,[6] values of k^isc were calculated, which are listed in Table 3 together with the ISC efficiencies, $p^\mathrm{isc} = k^\mathrm{isc}/k_{\mathrm{c,O_2}}^\mathrm{Q}$. The intercepts in Figure 4 are in reasonable agreement with the known values of $k_{\mathrm{A,O_2}}^\mathrm{Q}$.[17]

(c) Vibrational Relaxation of ND(c,v=1). Upon the addition of O_2 to vibrationally excited ND(c,v=1,J=1), emission from the vibrational ground state ND(c,v=0) was observed besides those of the (c,v=1 → a,v=1) and (A,v → X,v) transitions. Similar to equation 4, we obtain

$$\frac{N_{\mathrm{c},v=1}}{N_{\mathrm{c},v=0}} = \frac{\int_0^\infty [\mathrm{ND(c},v=1)]_t \mathrm{d}t}{\int_0^\infty [\mathrm{ND(c},v=0)]_t \mathrm{d}t} = \frac{k_{\mathrm{c},v=0}^\mathrm{rad} + k_{\mathrm{c},v=0}^\mathrm{pre} + k_{\mathrm{c},v=0,\mathrm{O_2}}^\mathrm{Q}[\mathrm{O_2}]}{k_{1,0}^\mathrm{vib}[\mathrm{O_2}]} \quad (5)$$

from the reaction scheme shown in Figure 5. The evaluation of eq 5 by spectra simulation yields the ratio $N_{\mathrm{c},v=1}/N_{\mathrm{c},v=0}$ as a function of $[O_2]^{-1}$, which is presented in Figure 6. The slope obtained by a least squares fit results in the rate constant for vibrational relaxation v=1 → v=0, $k_{1,0}^\mathrm{vib} = (0.6 \pm 0.1) \times 10^{-11}$ cm^3 s^{-1}. The intercept in Figure 6 corresponds to $k_{\mathrm{c},v=0,\mathrm{O_2}}^\mathrm{Q}/k_{1,0}^\mathrm{vib}$. This way, $k_{\mathrm{c},v=0,\mathrm{O_2}}^\mathrm{Q}$ is calculated to be $(10.5 \pm 1.1) \times 10^{-11}$ cm^3 s^{-1}, in good agreement with the values obtained in the time-resolved measurements (Table 1).

(d) Rotational Relaxation. Relaxation of the rotational population, NH/ND(c,v=0,J_i→J_f), was investigated for low rotational states J. For this purpose, each rotational state J was

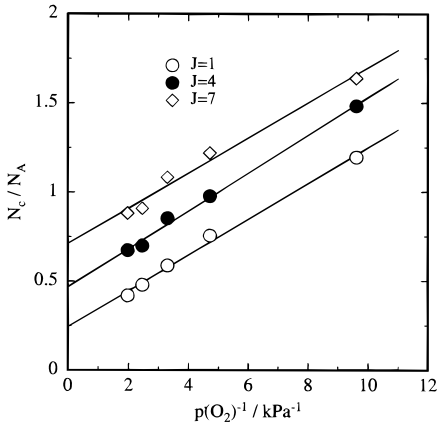

Figure 4. Ratio of the integrated c and A state concentrations of NH, $N_\mathrm{c}/N_\mathrm{A}$, as a function of the reciprocal of the O_2 pressure. The originally populated levels are J = 1, 4, and 7 of NH(c,v=0). The data for J = 4 and 7 are shifted by 0.25 and 0.5, respectively.

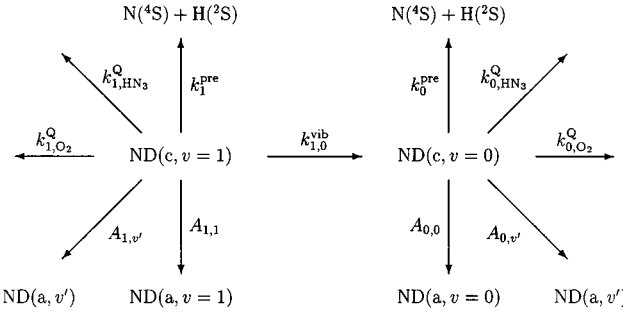

Figure 5. Reaction scheme of the relevant processes in the vibrational relaxation system ND(c,v=1) + O_2 → ND(c,v=0) + O_2. Here, $k_{1,\mathrm{O_2}}^\mathrm{Q}$ includes ISC to the A state and collisional removal to other electronic states. Electric dipole transitions to ND(b) are minor and not included in this scheme; Λ-doublets are not considered.

populated, and subsequently fluorescence spectra were taken in the presence of 104 Pa O_2. Single-collision rate constants for inelastic collisions with O_2 were derived by an iterative solution of the master equation

$$\frac{\mathrm{d}N_{u_\mathrm{m}}}{\mathrm{d}t} = N_{\mathrm{O_2}}\Big[\sum_{u_n \neq u_m}^{n_u} k_{u_n,u_m}^{\mathrm{O_2}} N_{u_\mathrm{n}}(t) - N_{u_\mathrm{m}}(t) \sum_{u_n \neq u_m}^{n_u} k_{u_m,u_n}^{\mathrm{O_2}}\Big] - N_{u_\mathrm{m}}(t)(k_{u_m}^\mathrm{rad} + k_{u_m}^\mathrm{pred} + N_{\mathrm{O_2}} k_{u_m}^\mathrm{Q}) \quad (6)$$

as described before for the systems NH/ND(c) + Ar and He,[9,10] NH(A) + He,[14] and PH(A) + He.[18] In comparison to the previously used form,[9,10,14,18] the last term of this master equation additionally takes care of the quenching by O_2. Equation 6 describes the change of the population N_{u_m} of a selected rotational state u_m by the processes $u_m \rightarrow u_n$ and $u_m \leftarrow u_n$ with time. Here, u_m and u_n present rotational states J in the presence

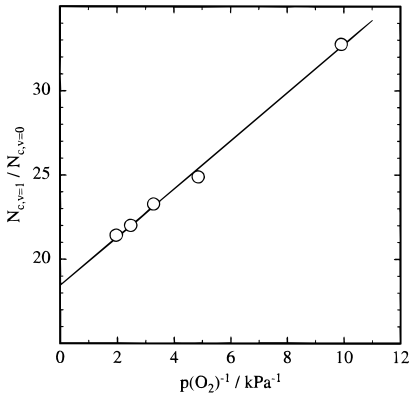

Figure 6. Ratio of the integrated $v=1$ and $v=0$ vibrational state concentration, $N_{c,v=1}/N_{c,v=0}$, of ND(c) for the initial population of ND-($c,v=0,J=1$) as a function of the inverse of the O_2 pressure.

TABLE 3: Rate Constants, k^{isc}, and Efficiencies, p^{isc}, of the Intersystem Crossing NH/ND($c,v,J\rightarrow A$) in Collisions with O_2 at Room Temperature

	v	J	$k^{isc}/(10^{-11}$ cm^3 cm$^{-1})$	p^{isc}
NH(c)	0	1	11.0 ± 1.1	0.45 ± 0.09
		4	10.4 ± 1.2	0.52 ± 0.05
		7	11.8 ± 1.4	0.78 ± 0.12
ND(c)	0	2	3.8 ± 0.9	0.31 ± 0.12
		4	3.9 ± 0.3	0.35 ± 0.04
		6	3.5 ± 0.2	0.32 ± 0.04
		8	3.6 ± 0.2	0.32 ± 0.03
ND(c)	1	1	5.5 ± 0.4	0.3 ± 0.1
		4	6.2 ± 0.3	0.3 ± 0.1

of the number density of O_2, N_{O_2}, and $k^Q_{u_m}$, the quenching rate constants as given in Table 1 by $k^Q_{c,O_2}(J)$. Instead of starting with arbitrary values, first input values for the desired single-collision state-to-state rate constants, $k^{O_2}_{u_m,u_n}$ and $k^{O_2}_{u_n,u_m}$, were obtained by neglecting multiple inelastic collisions.[9,14] In this case, the rate constants for the collisionally induced transitions from an initially pumped state u_m to state u_n are given by $k^{O_2}_{u_m,u_n} = (N_{u_n}/N_{u_m})/(N_{O_2}\tau_{u_m})$,[19] where $\tau^{-1}_{u_m} = k^{rad}_{u_m} + k^{pred}_{u_m} + N_{O_2} k^Q_{u_m}$, the sum of the decay rates by radiation, predissociation, and quenching of the originally excited state, which is known from ref 6 and this work. The further handling of eq 6 and, in particular, the evaluation of the fluorescence spectra have been described in detail before.[9,10,14,18] The resulting state-to-state rate constants for the relaxation of an initially populated state J_i to a final state J_f are summarized in Table 4 for NH($c,v=0,J$) and in Table 5 for ND($c,v=0,J$). We believe that the derived rate constants for $\Delta J = \pm 1$ transitions are precise within 10%−20%. The rate constants for $|\Delta J| > 1$ transitions are less precise.

(e) Electronic Quenching of ND(A,$v=0-3$). Table 2 shows that the product yields for the vibrational states ND(A,$v=0-3$) are alike. Time profiles of the Q-branches of the various $\Delta v=0$ (A→X) transitions were monitored at the wavelengths 335.6, 336.3, 337.2, and 338.5 nm for $v = 0$, 1, 2, and 3, respectively, using bandwidths of ±0.3 nm. At the selected wavelengths, the emission originates for more than 80% from the respective vibrational level. The ND(A) decays were evaluated at long fluorescence times for relatively high O_2 pressures (200−500 Pa), similar to the procedure applied before.[3] Rate constants for the quenching of ND(A,$v=0-3$) were estimated from plots of decay rates vs O_2 pressure to yield $k^{ND,Q}_{A,v} = (3.3 \pm 0.2)$, (3.9 ± 0.6), (4.2 ± 0.5), and $(4.4 \pm 0.7) \times 10^{-11}$ cm^3 s^{-1}, respectively. It should be noted that these estimates disregard vibrational relaxation by O_2. The intercepts of the plots result in values of ND(A,v) lifetimes, which are close to those reported in the literature,[7] but the present errors are significantly larger.

TABLE 4: Rate Constants at Room Temperature for the Rotational Relaxation of NH($c,v=0,J_i\rightarrow J_f$) by Collisions with O_2, $k_{J_i\rightarrow J_f}$: The Entry of Zero Means That the Constant Is Smaller Than 1×10^{-12} cm^3 s^{-1}; Rate Constants for Elastic Processes Were Not Determined in This Work

	$k_{J_i\rightarrow J_f}/10^{-11}$ cm^3 s^{-1} J_f								$\sum_{J_{f=1}}^{J_{max}} k_{J_i\rightarrow J_f}/$
J_i	1	2	3	4	5	6	7	8	10^{-11} cm^3 s^{-1}
1		8.7	3.8	1.8	0.1	0	0	0	14.4
2	6.8		7.2	2.6	0.8	0.3	0	0	17.7
3	3.2	7.7		5.9	1.4	0.4	0	0	18.6
4	2.1	3.7	7.8		4.5	1.2	0	0	19.3
5	0.2	1.9	2.9	7.3		3.3	0.8	0	16.4
6	0	0	1.7	3.6	6.3		2.7	0.6	14.9
7	0	0	0	0.2	3.3	6.0		2.5	12.0
8	0	0	0	0	0.3	3.3	6.3		9.9

The rate constants can be compared with that previously determined for NH(A,$v=2$), $k^{NH,Q}_{A,v=2} = (8.3 \pm 0.8) \times 10^{-11}$ cm^3 s^{-1}.[3]

Discussion

As mentioned in our previous studies on the kinetics of the NH/ND(c) relaxation,[9,10] we cannot resolve Λ-doublet states. All data given in this work hence refer to averages of the two Λ-doublet levels of the rotational states.

The competition of relaxation and quenching determines whether we can relate the observed quenching process to a single rotational state or to a more or less rotationally relaxed system. Literature data on the kinetics of rotational relaxation of NH/ND(c) by O_2 are not known to us. We will hence start with discussing the present data and recognize the following trends common to all three colliders Ar, He,[9,10] and O_2, which we have studied: The most dominant relaxation steps are those for $\Delta J = \pm 1$. While the efficiency for $\Delta J = -1$ steps stays approximately constant, it decreases with J for $\Delta J = +1$. Consequently, the latter process becomes less important for high J because of the increasing rotational energy splittings. Very much the same trends have been observed before for the rotational relaxation of PH($A^3\Pi,v=0$)[18] and NH($A^3\Pi,v=0$) by He,[14] if spin and Λ-doublet states are lumped together. The rate constants summed over all final states J_f, $\sum_{J_f=1}^{J_{max}} k_{J_i\rightarrow Jf}$ peak at about $J_i = 3$ for NH and 3−5 for ND, the thermally most likely populated states. The values for the highest rotational levels are found to be inherently too small, because the upward transitions had to be disregarded in the spectra evaluation. The relaxation of ND is faster than that of NH, again a correlation with the rotational splitting. The efficiency for rotational relaxation increases in the following order: He, Ar, O_2. The fastest constants being observed for the ND(c) + O_2 system exhibit sums of relaxation rate constants $\sum_{J_f=1}^{J_{max}} k_{J_i\rightarrow J_f}$ not far from collision frequency. One should further be aware that the evaluation requires the knowledge of the quenching rate constants $k^Q_{u_m}$ being dependent on $u_m = J$ as discussed below.

According to the exponential gap law, one can parametrize and fit the data of Tables 4 and 5 to the equation

$$k_{J_i\rightarrow J_f} = aR(\Delta E)(2J_f + 1)e^{-b|\Delta E/kT|} \qquad (7)$$

with $\Delta E = E_i - E_f$, the energy difference between the initial rotational state J_i and the final state J_f. This has been done before for the colliders Ar and He.[10] $R(\Delta E) = \Delta K_1(\Delta)e^{\Delta}$ is a dimensionless phase space factor expressed by $\Delta = (E_i - E_f)/(2kT)$ and $K_1(\Delta)$, a modified Bessel function of second kind and first order. Figure 7 shows the experimental data by plotting

TABLE 5: Rate Constants at Room Temperature for the Rotational Relaxation of ND(c,v=0,J_i→J_f) by Collision with O_2, $k_{J_i \to J_f}$: The Entry of Zero Means That the Constant Is Smaller than 1×10^{-12} cm^3 s^{-1}; Rate Constants for Elastic Processes Were Not Determined in This Work

	$k_{J_i \to J_f}/10^{-11}$ cm^3 s^{-1} J_f								$\sum_{J_{f=1}}^{J_{max}} k_{J_i \to J_f}/$
J_i	1	2	3	4	5	6	7	8	10^{-11} cm^3 s^{-1}
1		15.5	10.0	5.1	2.0	0	0	0	32.6
2	10.8		12.6	6.8	4.9	1.9	0.3	0	37.3
3	6.2	11.2		12.1	3.8	3.0	1.7	0	38.0
4	3.3	6.3	12.6		13.0	3.8	1.2	1.1	41.3
5	1.0	5.4	5.6	14.4		10.2	2.3	1.0	39.9
6	0	2.7	4.8	5.9	13.3		7.3	2.0	36.0
7	0	0	2.8	4.0	4.7	10.5		6.8	28.8
8	0	0	0	2.0	3.5	5.3	10.6		21.4

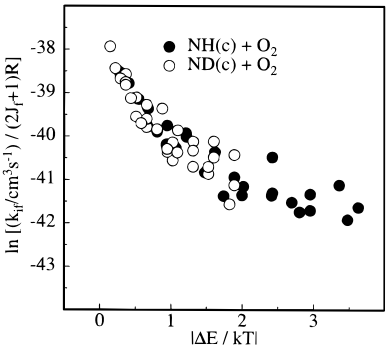

Figure 7. Exponential gap representation of the reduced rate constants for rotational relaxation of both isotopomers NH/ND(c,v=0). The resulting parameters a and b are listed in Table 6.

TABLE 6: Parameters a in Units 10^{-11} cm^3 s^{-1} and b (Dimensionless) Obtained in Fits of Eq 7 to the Data Displayed in Figure 7; The Last Column Gives the Energy Range of ΔE for Which the Parameters Are Valid

NH(c)		ND(c)		
a	b	a	b	$\Delta E/kT$
3.8 ± 1.6	2.3 ± 0.6	3.8 ± 1.4	2.4 ± 0.7	0−1
0.9 ± 0.5	0.7 ± 0.3	1.8 ± 1.5	0.9 ± 0.9	1−3.5

the logarithm of the rate constants, which have been divided by the statistical probability factor, $R(\Delta E)(2J_f + 1)$, vs the reduced energy gap $|\Delta E/kT|$. The parameters a and b in eq 7 can be fitted to the experimental data of $k_{J_i \to J_f}$. The resulting values are summarized in Table 6. As before for Ar and He,[10] two sets of parameters are given for each of the dependencies in Figure 7, namely, for the $\Delta E/kT$ range 0−1, which comprises the $\Delta J = \pm 1$ transitions, and $\Delta E > kT$, which takes care of steps $\Delta J > 1$. It is noteworthy that the data for both isotopomers are found to be essentially the same for this kind of representation.

At the beginning of this work, no J dependent quenching data were known to us. In the meantime Crosley and coworkers[20] have determined the values listed in Table 1 for NH(c,v=0). These constants are smaller than those of this work. The reason for this discrepancy is not evident, although triplet emission, if additionally received by the detector, might have lengthened the fluorescence decays. On the basis of our rotationally resolved rate data, we have calculated rate constants for the rotational temperature $T_{rot} = 300$ K[21,22] and obtain $k_{300K}^{NH,Q} = (20.9 \pm 0.4) \times 10^{-11}$ cm^3 s^{-1} for NH(c,v=0) and $k_{300K}^{ND,Q} = (11.7 \pm 0.3) \times 10^{-11}$ cm^3 s^{-1} for ND(c,v=0). This thermally averaged value of $k_{300K}^{NH,Q}$ is close to the corresponding values of Umemoto et al. [$(16.8 \pm 1.0) \times 10^{-11}$ cm^3 s^{-1}, if T = 300 K is assumed],[4] Rohrer and Stuhl [$(19.2 \pm 1.5) \times 10^{-11}$ cm^3 s^{-1}],[3] and Kenner et al. [$(19.6 \pm 1.0) \times 10^{-11}$ cm^3 s^{-1})].[23] Moreover, the quenching rate constants have been determined at 243 and 415 K to be (22.2 ± 1.6) and $(21 \pm 1) \times 10^{-11}$ cm^3 s^{-1}, respectively.[24] We hence prefer the present data. No value has been reported for ND(c) + O_2 yet. Previously, a near quantitative agreement for the quenching cross sections of NH(c) and OH(A) at room temperature has been observed.[23] Likewise we find that the isotope effects for the quenching of OH/OD(A)[22] and NH/ND(c) by O_2 are similar at room temperature. Furthermore both pairs of isotopomers show no significant temperature dependence of their rate constants when colliding with O_2.

The original aim of this work was to determine intersystem and quenching rate constants of NH/ND(c,v=0) as a function of rotational excitation. Colliding systems with small quenching efficiencies such as NH/ND(c) + Ar/He,[9,10] are ideal for relaxation but not for J specific quenching studies. On the other hand, if quenching is very fast compared to relaxation, the original rotational excitation of an isolated state becomes "frozen" and the J dependence of the quenching process can be advantageously investigated but not relaxation. In the present case of NH/ND(c), we have gotten hold of an ambiguous system in between these two extremes. This becomes apparent from the comparison of the data of Table 1 with those of Tables 4 and 5. While the total relaxation out of an originally excited J level of NH(c) is slightly less efficient than removal by quenching and fluorescence, it is relaxation that mainly removes the original rotational excitation of ND(c). Accordingly, experimental and simulated spectra show that the rotational excitation is partly relaxed before it is quenched. Under all experimental conditions, the originally populated rotational levels carry by far the highest population. In the case of NH, the adjacent rotational levels possess less than 20% of the initially excited level, with decreasing population for larger rotational steps. For ND we find the distribution of the time-integrated population to be significantly broader (adjacent levels less than 40%), as expected from the data of Tables 1 and 5. Nevertheless, the rotational distributions being quenched are markedly different for high and low rotational levels. We thus conclude that the quenching rate constants in Table 1 can be attributed mainly to the originally populated levels of NH(c) plus their much less populated neighboring levels and to significantly broadened distributions of ND(c). Besides this thermal averaging effect, one should keep in mind that the rotational energy of ND(c,v=0,J=8) is only half of that of NH(c,v=0,J=8). Within such a smaller energy range, the rotational effect probably is less pronounced. As a consequence of these two effects, only a very weak rotational dependence appears in Table 1 for the quenching of ND(c).

The data of Table 1 show that the rate constants decrease with increasing rotational energy. Such a trend has been observed before and has been attributed to an anisotropy of the relevant potential surfaces.[5,8,25] Rotation prevents the approaching colliders from adopting an optimal configuration. The independence of the rate constants of temperature results in decreasing cross sections with temperature. In the case of quenching of OH(A), this trend has been suggested to be due to attractive forces.[5,25,26] Because of the apparent similarity of the OH(A) quenching with that of the present system, the same explanation is likely, although calculated potential energy surfaces would give a more solid understanding of the dynamics. The observed rotational trend reverses that reported previously[3] for the relaxed (addition of Ar) and unrelaxed systems.

The rate constants $k_{u_m}^Q$ are identical with the rate constants k_{c,O_2}^Q of Table 1. The averaging effect by relaxation, i.e. the accuracy of k_{c,O_2}^Q for ND(c), influences the accuracy of the

relaxation data in Table 5 by the last term in eq 6. We expect the corresponding error not to be large for the deuterated system, because (i) this term is relatively small in comparison with the sum of all other removal terms in eq 6 and (ii) the variation in k^{Q}_{c,O_2} is small for NH(c) (not greater than ±23%) and is expected to be less for the more limited rotational energy range of ND(c).

The vibrational NH(A,v) product distributions in Table 2 display a significant dependence on the initially populated rotational level J for NH(c,v=0), but no rotational dependence at all for ND(c,v=0,1). Let us first note that the A state distributions are inconsistent with (c,v→A,v) Franck−Condon transitions. It has been noted in previous work on the NH system[3] that there are energy resonances for the spin conserving reactions Ia and Ib. More precise spectroscopic data indicate that these resonances with $O_2(a^1\Delta_g,v$=0,2,4) are slightly less close than calculated before.[3] First of all, one recognizes a more or less pronounced propensity to conserve the vibration of NH(c,v=0) and ND(c,v=0,1) similar to the trend to conserve rotation for the NH/ND(c,v=0→A,v=0) intersystem transitions. Common to these three collisionally induced Δv=0 transitions are near resonances with the energy for the formation of $O_2(b^1\Sigma^+_g,v$=0). With increasing rotational excitation of NH(c,v=0) we find an improving energy resonance for the intersystem crossing to NH(A,v=2) and the simultaneous excitation of $O_2(a^1\Delta_g,v$=0). This resonance picture, however, does not explain the marked vibrational excitation of ND(A,v) by ND(c,v=1) + O_2. It would be therefore desirable to study the dynamics of the NH/ND(c) system on the basis of calculated potential surfaces, which might help to understand the NH/ND(a) + O_2 → NH/ND(X) + O_2(b) system[27] as well.

Finally, the rate constants derived here for the ISC of NH(c,v=0) (Table 3) are close to those given by Okabe ($>12\times10^{-11}$ cm^3 s^{-1})[1] and Umemoto et al. [$(8.4\pm0.9)\times10^{-11}$ cm^3 s^{-1}][4] but significantly smaller than that previously reported by Rohrer and Stuhl [18×10^{-11} cm^3 s^{-1}].[3] Similarly in Table 3, the ISC efficiencies, p^{isc}, are close to the value given by Umemoto et al. (0.5)[4] for low J of NH(c,v=0). The rate constant and the ISC efficiency obtained previously in our laboratory[3] are too large, which is most likely due to the complicated evaluation procedure, which had to consider the photolytical formation of NH(A) as well. Although the overall quenching rate constants decrease, the intersystem crossing efficiency increases with J, as if an additional channel would become more accessible for this process. Perhaps this is due to the increasing resonance with $O_2(a^1\Delta_g,v$=0), as mentioned above. For all the investigated ND states, on the other hand, the ISC efficiencies stay near the value of one-third.

Acknowledgment. We thank L. Neitsch for numerous discussions concerning the evaluation of the data and D. R. Crosley for sending us the data of Table 1. We gratefully acknowledge financial support from the Deutsche Forschungsgemeinschaft (Grant No. Stu 59/31-1).

References and Notes

(1) Okabe, H. *J. Chem. Phys.* **1968**, *49*, 2726.
(2) Kawasaki, M.; Hirata, Y.; Tanaka, I. *J. Chem. Phys.* **1973**, *59*, 648.
(3) Rohrer, F.; Stuhl, F. *J. Chem. Phys.* **1987**, *86*, 226.
(4) Umemoto, H.; Kikuma, J.; Tsunashima, S.; Sato, S. *Chem. Phys.* **1988**, *123*, 159.
(5) Crosley, D. R. *J. Phys. Chem.* **1989**, *93*, 6273.
(6) Bohn, B.; Stuhl, F.; Parlant, G.; Dagdigian, P. J.; Yarkony, D. R. *J. Chem. Phys.* **1992**, *96*, 5059.
(7) Kenner, R. D.; Kaes, A.; Browarzik, R. K.; Stuhl, F. *J. Chem. Phys.* **1989**, *91*, 1440. Patel-Misra, D.; Parlant, G.; Sauder, D. G.; Yarkony, D. R.; Dagdigian, P. J. *J. Chem. Phys.* **1991**, *94*, 1913.
(8) Garland, N. L.; Crosley, D. R. *J. Chem. Phys.* **1989**, *90*, 3566.
(9) Yang, M.; Alexander, M. H.; Werner, H.-J.; Hohmann, J.; Neitsch, L.; Stuhl, F.; Dagdigian, P. J. *J. Chem. Phys.* **1995**, *102*, 4069.
(10) Hohmann, J.; Stuhl, F. *J. Chem. Phys.* **1996**, *105*, 3586.
(11) Bohn B.; Stuhl, F. *J. Phys. Chem.* **1993**, *97*, 4891.
(12) Bohn B.; Stuhl, F. *J. Phys. Chem.* **1993**, *97*, 7234.
(13) Altkorn, R. I.; Zare, R. N. *Annu. Rev. Phys.* **1984**, *35*, 265. Zare, R. N. *Angular Momentum*; Wiley: New York, 1988.
(14) Neitsch, L.; Stuhl, F.; Dagdigian, P. J.; Alexander, M. H. *J. Chem. Phys.* **1996**, *104*, 1325.
(15) Brazier, C. R.; Ram, R. S.; Bernath, P. F. *J. Mol. Spectrosc.* **1986**, *120*, 381.
(16) Patel-Misra, D.; Sauder, D. G.; Dagdigian, P. J. *Chem. Phys. Lett.* **1990**, *174*, 113.
(17) Kenner, R. D.; Kaes, A.; Browarzik, R. K.; Stuhl, F. *J. Chem. Phys.* **1989**, *91*, 1440.
(18) Neitsch, L.; Stuhl, F.; Dagdigian, P. J.; Alexander, M. H. *J. Chem. Phys.* **1997**, *106*, 7642.
(19) Bergmann, K.; Demtröder,W. *Z. Phys.* **1971**, *243*, 1.
(20) Crosley, D. R. Private communication, 1996.
(21) Copeland, R. A.; Crosley, D. R. *J. Chem. Phys.* **1986**, *84*, 3099.
(22) Kenner, R. D.; Capetanakis, F. P.; Stuhl, F. *J. Phys. Chem.* **1990**, *94*, 2441.
(23) Kenner, R. D.; Rohrer, F.; Stuhl, F. *J. Phys. Chem.* **1989**, *93*, 7824.
(24) Kenner, R. D.; Pfannenberg, S.; Heinrich, P.; Stuhl, F. *J. Phys. Chem.* **1991**, *95*, 6586.
(25) Copeland, R. A.; Dyer, M. J.; Crosley, D. R. *J. Chem. Phys.* **1985**, *82*, 9.
(26) Copeland, R. A.; Crosley, D. R. *Chem. Phys. Lett.* **1984**, *107*, 295.
(27) Bohn, B.; Stuhl, F. *J. Chem. Phys.* **1995**, *102*, 618.